Outgoing excitonic resonance in multiphonon Raman scattering from polar semiconductors

V. I. Belitsky, A. Cantarero, and S.T. Pavlov*
Departamento de Física Aplicada, Universidad de Valencia, Burjasot, E-46100 Valencia, Spain

M. Cardona
Max Planck Institut für Festkörperforschung, Heisenbergstrasse 1, D-70569 Stuttgart, Germany

I. G. Lang and A. V. Prokhorov
A. F. Ioffe Physico-Technical Institute, Russian Academy of Sciences, 194021 St. Petersburg, Russia
(Received 14 June 1995)

The theory of scattering process involving both free electron-hole pairs (EHP's) and Wannier-Mott excitons as intermediate states is developed for high-order multiphonon resonant Raman scattering (MPRRS) from polar semiconductors. The combined scattering mechanism removes the disagreement between experiment and theory which appears in the model of MPRRS via high-energy states of discrete excitons because of the hot exciton instability to decay. The binding of free EHP's into the exciton at the last stage of the process explains both the outgoing excitonic resonance and the small decrease in the peak amplitude with the number of phonons observed for high-order MPRRS. The profile of the outgoing excitonic resonance must be asymmetric because of the strong increase in exciton lifetime below the resonance.

I. INTRODUCTION

The spectra[1–6] of multiphonon resonant Raman scattering (MPRRS) from bulk semiconductors (CdS, CdSe, ZnO, ZnS, ZnSe, ZnTe, GaP, InAs, InBr, and InI) exhibit a so-called outgoing excitonic resonance, i.e., an enhancement of the peak intensity when the scattered light frequency $\omega_s = \omega_l - N\omega_{\rm LO}$ approaches the energy $E_{\rm ex} = \hbar\omega_{\rm ex}$ of the exciton ground state. Hence, the MPRRS theory should incorporate the states of excitons as intermediate states in the scattering process. However, such theory (see Refs. 7–9), when using only discrete excitonic states, predicts a rather rapid decrease in the maximum of scattering intensity with the increase of N when the decay of those discrete excitonic states into the continuum is taken into account. This result is in strong disagreement with experiment where up to 20 phonon replicas have been observed[1–6] (e.g., $N = 9$ for CdS and $N = 20$ for InI and InBr).

The MPRRS process via the discrete part of the excitation spectrum can be described as follows: The incident photon creates a Wannier-Mott hot exciton via an indirect, LO-phonon-assisted transition. After that, the exciton emits successively $N-2$ LO phonons, reducing the energy by $\hbar\omega_{\rm LO}$ in every step of the cascade process. The process ends with the indirect exciton recombination involving the emission of the last LO phonon and a light quantum $\hbar\omega_s$. The cross section $\sigma_N^{\rm ex}$ of such a process[10] is proportional to the first power of the Fröhlich electron-LO phonon coupling constant α for arbitrary N. The increase in N by 1 gives rise to a factor $\gamma_s/\gamma_{\rm ex}$ in the expression for $\sigma_N^{\rm ex}$, where $\gamma_{\rm ex} \simeq \gamma_s + \gamma_d$ is the total inverse lifetime of the exciton with γ_d and γ_s the probability of scattering into the continuum (exciton decay) and discrete states, respectively. It was shown[7] that for $m_e \ll m_h$, where m_e (m_h) is the effective mass of the electron (hole), the factor $\gamma_s/\gamma_{\rm ex} \simeq 1/2$ while for $m_e \sim m_h$, $\gamma_s/\gamma_{\rm ex} \ll 1$. With increasing N the factors of order $\gamma_s/\gamma_{\rm ex} < 1$ accumulate; this should lead to a rapid decrease in $\sigma_N^{\rm ex}$. In this case the theory of MPRRS via the discrete states of excitons fails to account for the observation of processes involving *large* N.

On the other hand, the MPRRS efficiency for scattering via the states of uncorrelated electron-hole pairs (EHP's) is free from such reduction parameters.[11–13] Qualitatively, the negligibly small value of the counterpart of γ_d in the probability of cascade scattering via free pairs prevents the cross section from a rapid decrease with N. The cross section $\sigma_N^{\rm EHP}$ is proportional to α^3 for $N \geq 4$.[11,12] However, *this mechanism cannot explain the strong outgoing resonance* found for $\omega_s = \omega_{\rm ex}$.[14]

Thus, it is tempting to combine the scattering via the states of free EHP's (exciton continuum) with that via the discrete states of a Wannier-Mott exciton to account for the observation of high-order replicas in MPRRS along with the outgoing excitonic resonance. The important role of the continuum for two-LO-phonon scattering was demonstrated in Ref. 15. Another indication of the importance of the continuum follows from the theory of a monomolecular creation of the discrete excitons from hot EHP's.[16,17] In a monomolecular process a discrete exciton is created by the hot electron and hole, which are simultaneously excited by the light at the same point of a crystal and preserve their spatial correlation until the last step of the process when they bind into the exciton after being cooled by the emission of a number of LO phonons. The initial stages of the process, the direct cre-

ation of a hot EHP and the successive emission of $N-1$ phonons, are the same as in MPRRS via free EHP's.

II. SCATTERING EFFICIENCY

In this paper we demonstrate that the combined scattering via the states of free EHP *and* discrete excitons *resolves the discrepancy between the theory and experiment for large* N. The relevant diagrams for MPRRS efficiency are given in Fig. 1, where the processes with one [Fig. 1(a)] and two [Fig. 1(b)] excitonic intermediate states at the last stage of the MPRRS process are shown. In the range of outgoing resonance *only these two diagrams* correspond to processes in which the discrete exciton cannot decay into the continuum via emission of a LO phonon. A schematic representation of both processes is given in Fig. 2, where the thick line RR' shows the initial excitation level corresponding to the excitonic outgoing resonance. The contribution of a process in Fig. 1(a) to the outgoing resonance corresponds to the cascade of $(N-1)$ transitions [from E to F in Fig. 2(a)] via the states of the continuum followed by LO-phonon-assisted recombination via the discrete exciton state P. Similarly, the resonant contribution of the diagram in Fig. 1(b) corresponds to the process with $(N-2)$ transitions [from K to T in Fig 2(b)] involving the exciton continuum, followed by the binding into the discrete exciton state Q and an LO-phonon-assisted recombination via the state S. Other details of Fig. 2 will be discussed later.

To simplify calculations we use the plane-wave approximation for the states of the exciton continuum. This approximation, being valid for high-energy states, may lead to errors in the contribution of continuous states close to the fundamental gap. However, for large N the relative weight of this contribution should become small. A more detailed calculation involving continuous excitonic states is required to assess the magnitude of the errors committed in the plane-wave approximation.

The MPRRS cross section can be written as[10,18]

$$\frac{d^2\sigma}{dod\omega_s} = \frac{\omega_s^3\omega_l V_0}{c^4}\frac{n_s}{n_l}e^*_{s\alpha}e_{s\beta}e_{l\gamma}e^*_{l\lambda}S_{\alpha\gamma\beta\lambda}(\omega_l,\omega_s,\kappa_l,\kappa_s) = \frac{V_0^2\omega_s^2 n_s^2}{(2\pi)^3c^3u_l u_s}\bar{W}_s, \quad (1)$$

where $S_{\alpha\gamma\beta\lambda}$ is the light-scattering tensor of rank four, V_0 the normalization volume, c the light velocity in vacuum, and n_l (n_s), $\mathbf{e}_l$ ($\mathbf{e}_s$), κ_l (κ_s), and u_l (u_s) are the refractive index, the polarization vector, the wave vector, and the group velocity of the incident (scattered) light, respectively. $\bar{W}_s$ is the scattered light emission probability per unit time, normalized to one photon of incident radiation.

From here on, we make the additional assumption that the effective mass of the hole is much larger than that of the electron.[19] This lets us select only those contributions to the scattered intensity where all phonons, emitted before coupling of an EHP into the exciton, are emitted by the electron (see Fig. 1): the energy of the hole generated near the resonance is not enough for emission of an LO phonon in a real transition.

A. Contribution of type *a*

In accordance with the diagrammatic rules[10,12] for $S_{\alpha\gamma\beta\lambda}$, the contribution of the diagram in Fig. 1(a) can be written as

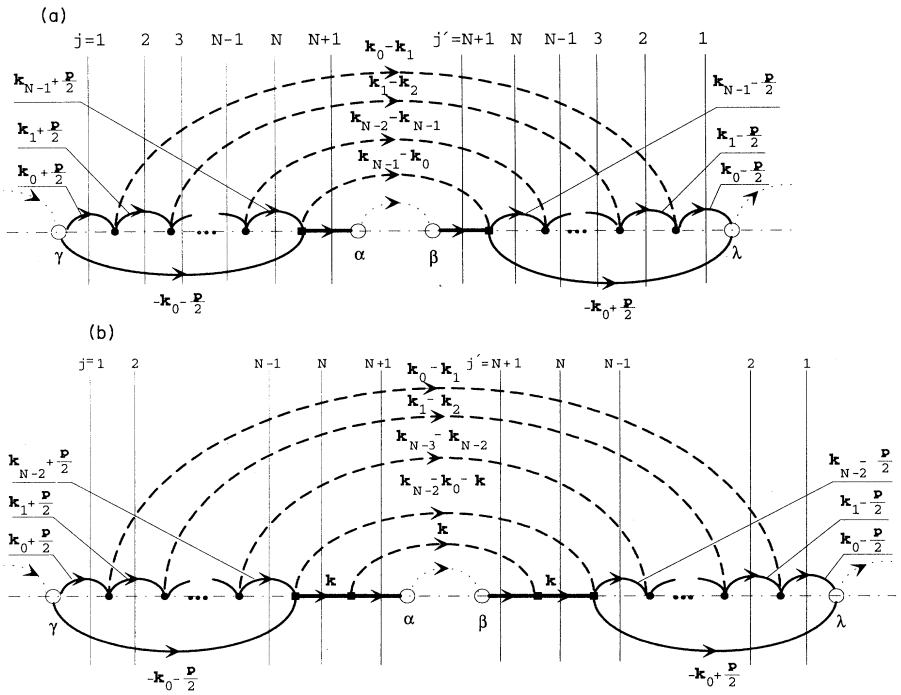

FIG. 1. The diagrams with (a) one and (b) two discrete exciton intermediate states (thick solid lines) contributing to the MPRRS efficiency in the range of outgoing resonance. Empty (filled) circles correspond to the electron-photon (electron-LO phonon) interactions while the square vertices are shown for transitions between two states of the discrete exciton and for discrete-continuum transitions. Thin solid and thick dashed lines represent electron-hole pairs and LO phonons, respectively.

$$S^{aN}_{\alpha\gamma\beta\lambda} = \frac{J^*_\alpha J_\beta J_\gamma J^*_\lambda}{\pi a^3 \omega_s^2 \omega_l^2 \hbar^{2N+2}} \frac{\delta(\omega_l - \omega_s - N\omega_{\rm LO})}{(\omega_s - \omega_{\rm ex})^2 + [\gamma_{\rm ex}(0)/2]^2} \sum_{\mathbf{k}_0 \mathbf{k}_1 \ldots \mathbf{k}_{n-1}, \mathbf{p}} \left[\prod_{j=0}^{N-1} |C_{\mathbf{k}_j - \mathbf{k}_{j+1}}|^2 \right] M_{\mathbf{k}0}(\mathbf{k}_{N-1} - \mathbf{k}_0) M^*_{\mathbf{k}'0}(\mathbf{k}_{N-1} - \mathbf{k}_0)$$
$$\times \Theta_{N-1}(\mathbf{k}_0, \mathbf{k}_1, \ldots, \mathbf{k}_{N-1}, \mathbf{p}) \Theta^*_{N-1}(\mathbf{k}_0, \mathbf{k}_1, \ldots, \mathbf{k}_{N-1}, -\mathbf{p}), \tag{2}$$

where $\mathbf{k}_N \equiv \mathbf{k}_0$, $\mathbf{k} = \mathbf{k}_{N-1}(m_h/M) + \mathbf{k}_0(m_e/M) + \mathbf{p}/2$, $\mathbf{k}' = \mathbf{k}_{N-1}(m_h/M) + \mathbf{k}_0(m_e/M) - \mathbf{p}/2$, $\Theta_{N-1}(\mathbf{k}_0, \mathbf{k}_1, \ldots, \mathbf{k}_{N-1}, \mathbf{p})$ is the factor containing the energy denominators of all vertical sections from $j = 1$ to $j = N$ in the diagram of Fig. 1(a), $J_\gamma = (e/m_0)p_{cv,\gamma}$, a is the exciton Bohr radius, $C_{\mathbf{q}} = -i\hbar\omega_{\rm LO}\sqrt{4\pi\alpha l^3/V_0}(lq)^{-1}$ represents the Fröhlich interaction, $l = \sqrt{\hbar/2m_e\omega_{\rm LO}}$, $M_{\mathbf{k}0}(\mathbf{q}) = \langle 0|\exp(-i\mathbf{q}\rho m_h/M) - \exp(i\mathbf{q}\rho m_e/M)|\mathbf{k}\rangle$ is the matrix element for transitions between uncorrelated continuous and discrete states of the exciton with the emission of LO phonon, and ρ is the relative motion coordinate. In the limit $m_h \gg m_e$,

$$\Theta_{N-1}(\mathbf{k}_0, \mathbf{k}_1, \ldots, \mathbf{k}_{N-1}, \mathbf{p}) \simeq \left(-\frac{2m_e}{\hbar}\right)^N \prod_{j=0}^{N-1} [(\mathbf{k}_j + \mathbf{p}/2)^2 - K_j^2 - iQ_j^2]^{-1}, \tag{3}$$

where $K_j = \sqrt{(2m_e/\hbar)(\omega_l - \omega_g - j\omega_{\rm LO})}$ and $Q_j^2 = (m_e/\hbar)\gamma_e(\mathbf{K}_j)$. The resonant factor $\{(\omega_s - \omega_{\rm ex})^2 + [\gamma_{\rm ex}(0)/2]^2\}^{-1}$ is due to the two vertical sections $j = N+1$ and $j' = N+1$ in the left and right parts of the diagram, respectively.

Substituting Eq. (3) into Eq. (2) and integrating over the absolute value of wave vectors $\mathbf{k}_0, \mathbf{k}_1, \ldots, \mathbf{k}_{N-1}$ we find

$$S^{aN}_{\alpha\gamma\beta\lambda} = J^*_\alpha J_\beta J_\gamma J^*_\lambda Z_N(\eta) \frac{\alpha^3 \delta(\omega_l - \omega_s - N\omega_{\rm LO})}{l^3 \pi^{N+3} 2^{2N-3} (\hbar\omega_l \omega_s)^2} \frac{[(1 + K_0^2 a^2)^{-2} - (1 + K_{N-1}^2 a^2)^{-2}]^2}{(\omega_s - \omega_{\rm ex})^2 + [\gamma_{\rm ex}(0)/2]^2}, \tag{4}$$

$$Z_N(\eta) = \alpha^{N-3} l^{-N+3} \int d\mathbf{p} \prod_{j=0}^{N-1} dO_j [l^2 |\mathbf{K}_j - \mathbf{K}_{j+1}|^2 (\lambda_j^{-1} + ip\cos\vartheta_j)]^{-1}, \tag{5}$$

$\eta = \omega_{\rm LO}/(\omega_l - \omega_g)$, $\mathbf{K}_N \equiv \mathbf{K}_0$, the direction of $\mathbf{K}_j$ is determined by the solid angle O_j, ϑ_j is the angle between $\mathbf{K}_j$ and $\mathbf{p}$, and $\lambda_j = \hbar K_j/m_e\gamma_e(K_j)$. The wave vector $\mathbf{p}$ corresponds to the uncertainty in the quasimomentum of the relative motion of an electron and hole.[12] According to the uncertainty principle $p \simeq 1/\Delta r$, where Δr is the size of an EHP,[12] which is proportional to the electron mean free path $\lambda = v\tau = \hbar K/m_e\gamma_e$. This leads to the estimate $p \simeq \lambda^{-1}$, which has allowed us to use the relation $pa \ll 1$ in Eq. (4) under the assumption that the exciton radius a is smaller than the electron mean free path λ. The constraint $pa \ll 1$ is not obligatory but Eq. (4) would be more complicated without it.

The inverse lifetime of the electron for scattering by LO phonons is given by

$$\gamma_e(k) = \begin{cases} \Gamma_e(k), & E < \hbar\omega_{\rm LO}; \\ 2\alpha\omega_{\rm LO}(\hbar\omega_{\rm LO}/E)^{1/2} \cosh^{-1}(E/\hbar\omega_{\rm LO})^{1/2}, & E > \hbar\omega_{\rm LO}, \end{cases} \tag{6}$$

where $E = \hbar^2 k^2/2m_e$ and $\Gamma_e(k) \ll \alpha\omega_{\rm LO}$ is determined by interaction with acoustic phonons or impurities.

Substitution of Eq. (6) into Eq. (5) leads to

$$Z_N(\eta) = \eta^3 (\cosh^{-1}\eta^{-1/2})^{-N+3} \int d\mathbf{x} \prod_{j=0}^{N-1} dO_{\mathbf{y}_j} |\mathbf{y}_j - \mathbf{y}_{j+1}|^{-2} \frac{\gamma_j/\gamma_0 y_j - ix\cos\vartheta_j}{x^2\cos^2\vartheta_j + (\gamma_j/\gamma_0 y_j)^2}, \tag{7}$$

where $\mathbf{y}_N \equiv \mathbf{y}_0$, the dimensionless vectors $\mathbf{x} = \lambda_0\mathbf{p}$ and $\mathbf{y}_j = l\sqrt{\eta}\mathbf{K}_j$, $y_j = \sqrt{1 - j\eta}$ and

$$\frac{\gamma_j}{\gamma_0} \equiv \frac{\gamma_e(K_j)}{\gamma_e(K_0)} = \begin{cases} y_j^{-1} \cosh^{-1}(y_j/\sqrt{\eta})/\cosh^{-1}(1/\sqrt{\eta}), & 0 < \eta < (j+1)^{-1}; \\ \Gamma_e(K_j)/\gamma_0, & \eta > (j+1)^{-1}. \end{cases}$$

Equation (7) proves that the value $Z_N(\eta)$ is independent of the Fröhlich constant α, a fact that clarifies the dependence on α in Eq. (4).

B. Contribution of type *b*

We proceed to evaluate the contribution of a process in Fig. 1(b). Using the same scheme as for the process of Fig. 1(a) we find

$$S^{bN}_{\alpha\gamma\beta\lambda} \simeq J^*_\alpha J_\beta J_\gamma J^*_\lambda \frac{\alpha^3\delta(\omega_l-\omega_s-N\omega_{\rm LO})}{l^3(\hbar\omega_l\omega_s)^2\{(\omega_s-\omega_{\rm ex})^2+[\gamma_{\rm ex}(0)/2]^2\}}\frac{2M}{m_e}\frac{\alpha\omega_{\rm LO}}{\gamma_{\rm ex}(K^{\rm ex}_{N-1})}\frac{|M_{00}(K^{\rm ex}_{N-1})|^2}{\pi^{N+3}2^{2N-3}}$$
$$\times\int dO_0 dO_{N-2} dO^{\rm ex}_{N-1}\Phi_{N-1}(O_0,O_{N-2},O^{\rm ex}_{N-1})Z^{\rm ex}_{N-1}(O_0,O_{N-2},O^{\rm ex}_{N-1}), \tag{8}$$

where

$$|M_{00}(K)|^2=\left\{\left[1+\left(\frac{m_h}{2M}Ka\right)^2\right]^{-2}-\left[1+\left(\frac{m_e}{2M}Ka\right)^2\right]^{-2}\right\}^2,$$

$$\Phi_{N-1}(O_0,O_{N-2},O^{\rm ex}_{N-1})=\left\{\left[1+\left(\mathbf{K}_0+\frac{m_h}{M}\mathbf{K}^{\rm ex}_{N-1}\right)^2a^2\right]^{-2}-\left[1+\left(\mathbf{K}_{N-2}-\frac{m_e}{M}\mathbf{K}^{\rm ex}_{N-1}\right)^2a^2\right]^{-2}\right\},$$

$$Z^{\rm ex}_{N-1}(O_0,O_{N-2},O^{\rm ex}_{N-1})=\frac{\alpha^{N-4}}{l^{N-4}}\int\prod_{j=1}^{N-3}dO_j[l^2|\mathbf{K}_{j-1}-\mathbf{K}_j|^2]^{-1}[l^2|\mathbf{K}_{N-3}-\mathbf{K}_{N-2}|^2l^2|\mathbf{K}_{N-2}-\mathbf{K}_0-\mathbf{K}^{\rm ex}_{N-1}|]^{-1}$$
$$\times\int d\mathbf{p}\prod_{j=0}^{N-2}[(\lambda_j^{-1}+ip\cos\vartheta_j)]^{-1} \tag{9}$$

and $K^{\rm ex}_{N-1}=\sqrt{(2M/\hbar)\,[\omega_l-\omega_{\rm ex}-(N-1)\omega_{\rm LO}]}$ is the absolute value of the exciton wave vector at the penultimate state.

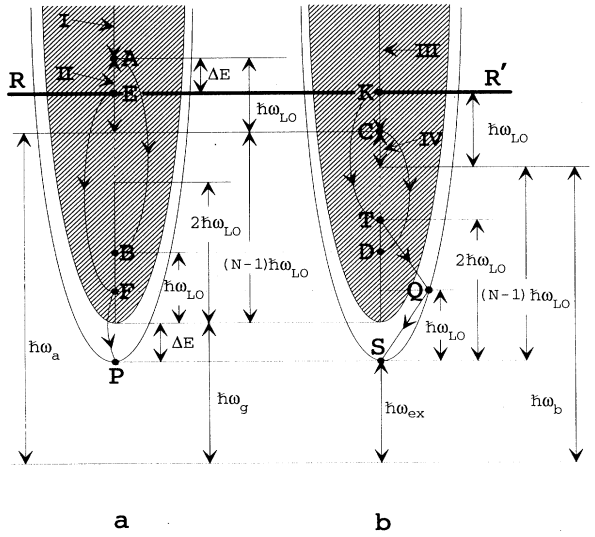

a b

FIG. 2. Schematic representation of processes contributing to the outgoing excitonic resonance and corresponding (a) to the diagram in Fig. 1(a) and (b) to that in Fig. 1(b), respectively. The thick line RR' corresponds to the resonant incident frequency $\omega_l=\omega_{\rm ex}+N\omega_{\rm LO}$. The frequency intervals I, II, III, and IV are defined with respect to the scattering mechanism responsible for the finite lifetime of the last free EHP intermediate state before binding into the exciton. N out of $N+1$ intermediate states are real in the interval I+II (III+IV) for the process in Fig. 1(a) [Fig. 1(b)]. See text for details.

C. Expression via the distribution function

The results for the scattering processes of Fig. 1 can be written in terms of the distribution function of EHP's with respect to the relative distance between electron and hole participating in the initial stage of the MPRRS process. Such a function $f_N(\mathbf{r})$ for free EHP's after emission of N LO phonons has been introduced in Ref. 12. For a simplified model of electron-phonon interaction[11] $C^Z_{\mathbf{q}}=-i\hbar\omega_{\rm LO}\sqrt{4\pi\tilde{\alpha}l^3/V_0}=lqC_{\mathbf{q}}$, which is similar to the deformation potential, and in the limit $m_h\gg m_e$, $f_N(\mathbf{r})$ is given by

$$f^Z_N(\mathbf{r})=\int d^3\mathbf{r}_1\cdots\int d^3\mathbf{r}_N W_0(\mathbf{r}_1)$$
$$\times W_1(\mathbf{r}_2-\mathbf{r}_1)\cdots W_N(\mathbf{r}-\mathbf{r}_N), \tag{10}$$

where $W_j(\mathbf{r})=(4\pi\lambda_j r^2)^{-1}\exp(-r/\lambda_j)$, $\int d\mathbf{r}f^Z_N(\mathbf{r})=1$. The total number n_N of EHP's after emission of N phonons,[12] normalized to one incident photon, and in the limit $m_h\gg m_e$, is $n_N=W_l/\gamma_e(K_N)$, where

$$W_l=\frac{V_0|M_l|^2m_e}{\pi\hbar^3}\left[\frac{2m_e}{\hbar}(\omega_l-\omega_g)\right]^{1/2},$$
$$M_l=-\frac{e}{m_0}\mathbf{e}_l\mathbf{p}_{cv}\left(\frac{2\pi\hbar u_l}{V_0cn_l\omega_l}\right)^{1/2} \tag{11}$$

are the probability of direct EHP creation per photon and the matrix element of the electron-photon interaction, respectively.

Using Eqs. (1), (4), (10), and (11) leads to the contribution of the diagram in Fig. 1(a)

$$\bar{W}^{aZ}_{sN}=n^Z_{N-1}f^Z_{N-1}(\mathbf{r}=0)V_0W^Z_{AN}, \tag{12}$$

where

$$W_{AN}^{Z} = \frac{\tilde{\alpha}\omega_{\mathrm{LO}}^{2}|M_s|^2\pi^2\delta(\omega_l-\omega_s-N\omega_{\mathrm{LO}})}{2^{-9}\hbar^2\{(\omega_s-\omega_{\mathrm{ex}})^2+[\gamma_{\mathrm{ex}}(0)/2]^2\}} \times[(1+K_0^2a^2)^{-2}-(1+K_{N-1}^2a^2)^{-2}]^2 \quad (13)$$

is the probability of phonon-assisted EHP recombination via the discrete exciton state and M_s is given by Eq. (11) after changing the index l for s.

It follows from Eq. (12) that the probability of scattered light emission is proportional to the normalized EHP distribution function $f_{N-1}^{Z}(\mathbf{r}=0)$ at zero relative distance. This result has been obtained under the assumption $pa \ll 1$, which is equivalent to $\lambda \gg a$ and means that the linear dimension of the exciton is small in comparison with that of the EHP. Then the binding of an EHP into an exciton happens basically for $\mathbf{r}=0$.

In a similar way, the contribution of a diagram in Fig. 1(b) for the model interaction is

$$\bar{W}_{sN}^{bZ} = n_{N-2}^{Z} f_{N-2}^{Z}(\mathbf{r}=0)V_0 W_{BN-1}^{Z}\frac{\gamma_l^Z(K_{N-1}^{\mathrm{ex}})}{\gamma_{\mathrm{ex}}^Z(K_{N-1}^{\mathrm{ex}})}, \quad (14)$$

where W_{BN-1}^{Z} is the number of EHP transitions per unit time into an exciton in a volume V_0, when the wave vectors of electron and hole are $\mathbf{K}_{N-2}$ and $-\mathbf{K}_0$, respectively. To lowest order in $\tilde{\alpha}$ we find

$$W_{BN-1}^{Z} = \tilde{\alpha}\omega_{\mathrm{LO}}\frac{a^3}{V_0}\frac{M}{m_e}lK_{N-1}^{\mathrm{ex}}2^5\int dO_{N-1}^{\mathrm{ex}}\{[1+(\mathbf{K}_0+\mathbf{K}_{N-1}^{\mathrm{ex}})^2a^2]^{-2}-[1+K_{N-2}^2a^2]^{-2}\}^2. \quad (15)$$

In the right-hand side of Eq. (14) $\gamma_l^Z(K_{N-1}^{\mathrm{ex}})$ is the probability of indirect emission of a photon by the exciton with the wave vector $\mathbf{K}_{N-1}^{\mathrm{ex}}$ via the intermediate exciton state with $K^{\mathrm{ex}}=0$. Second-order perturbation theory leads to

$$\gamma_l^Z(K_{N-1}^{\mathrm{ex}}) = \frac{8\pi\tilde{\alpha}\omega_{\mathrm{LO}}^2l^3}{\hbar^2a^3}|M_s|^2|M_{00}(K_{N-1}^{\mathrm{ex}})|^2\frac{\delta(\omega_l-\omega_s-N\omega_{\mathrm{LO}})}{(\omega_s-\omega_{\mathrm{ex}})^2+[\gamma_{\mathrm{ex}}(0)/2]^2}. \quad (16)$$

D. Limits of applicability

The results for combined contributions to the MPRRS efficiency in Eqs. (4) and (8) or, equivalently, Eqs. (12) and (14), describe the cascade-type of scattering process that includes a number of transitions via *real intermediate states*. This raises the question of the limits of applicability of those equations.

Equation (4) is valid for $N \geq 4$ in the interval $\omega_l > \omega_a = \omega_g + (N-1)\omega_{\mathrm{LO}}$, where all intermediate states of the free EHP's are real. This interval can be divided into two subintervals (I) $\omega_l > \omega_g + N\omega_{\mathrm{LO}}$ and (II) $\omega_g + (N-1)\omega_{\mathrm{LO}} < \omega_l < \omega_g + N\omega_{\mathrm{LO}}$, as shown in Fig. 2(a). All the inverse lifetimes $\gamma_e(K_0),\ldots,\gamma_e(K_{N-1})$ of EHP's in the intermediate states are determined by the probability for an electron to emit an LO phonon in the real transition in the subinterval (I) whereas in (II) the energy of an electron with the wave vector K_{N-1} is not enough for LO phonon emission. Therefore in interval (II) the value $\gamma_e(K_{N-1}) = \Gamma_e(K_{N-1})$ [see Eq. (6)] is determined by other mechanisms which are *weak* compared to the Fröhlich interaction. One can then expect the scattering efficiency to show some characteristic feature when the laser frequency goes through the point A, where $\omega_l = \omega_g + N\omega_{\mathrm{LO}}$, and the energy of the electron in the state K_{N-1} crosses the point B placed one LO phonon above the fundamental gap. However, the strong change in the value of the electron lifetime $\gamma_e(K_{N-1}) \to \Gamma_{N-1}(K_{N-1})$ does not lead to any resonance in the scattering efficiency because of the compensation discussed below.

Equation (8) is valid for $N \geq 5$ in the interval $\omega_l > \omega_b = \omega_{\mathrm{ex}} + (N-1)\omega_{\mathrm{LO}}$, where $N-1$ intermediate states of free EHP's and the discrete exciton state with the wave vector K_{N-1}^{ex} in a cascade of transitions after absorption of the incident photon are real. This interval corresponds to the two subintervals (III) $\omega_l > \omega_g + (N-1)\omega_{\mathrm{LO}}$ and (IV) $\omega_{\mathrm{ex}} + (N-1)\omega_{\mathrm{LO}} < \omega_l < \omega_g + (N-1)\omega_{\mathrm{LO}}$ as shown in Fig. 2(b). For the frequency interval (III) $\gamma_e(K_0),\ldots,\gamma_e(K_{N-2})$ are determined by the emission of an LO phonon whereas in (IV) $\gamma_e(K_{N-2}) \to \Gamma_e(K_{N-2})$. Again, one can expect some qualitative change to happen when ω_l goes through the point C, where $\omega_l = \omega_g + (N-1)\omega_{\mathrm{LO}}$, and the energy of the electron in the state K_{N-2} crosses the point D in Fig. 2(b).

The limits of applicability of Eqs. (4) and (8) with respect to the scattering order N are determined by the convergence of integral over p in Eqs. (5) and (9) for large p.

III. DISCUSSION AND CONCLUSIONS

We have now all necessary equations to discuss the relative importance of the two contributions in Fig. 1 and to compare them with that for the scattering via free EHP's only. The light scattering tensor for the MPRRS via free EHP's was analyzed in Ref. 12. It was shown that the main contribution corresponds to processes with one virtual intermediate state. The minimal energy detuning[12] in this virtual state is equal to $\hbar\omega_{\mathrm{LO}}$. Following Eq. (1) and Ref. 12 we can write

$$S_{\alpha\gamma\beta\lambda}^{N} = J_\alpha^* J_\beta J_\gamma J_\lambda^* \frac{\alpha^3\delta(\omega_l-\omega_s-N\omega_{\mathrm{LO}})}{2^{-3}l^3\omega_{\mathrm{LO}}^2(4\pi)^{N+3}} \times(1-1/N)^2\{Z_N(\eta)+Z_N[\eta/(1-\eta)]\} \quad (17)$$

or, similar to Eqs. (12) and (14),

$$\bar{W}^Z_{sN} = n^Z_N(\mathbf{k}=0) f^Z_N(\mathbf{k}=0, \mathbf{r}=0) V_0 W_C, \qquad (18)$$

where $W_C = (2\pi/\hbar)|M_s|^2 \delta(\hbar\omega_l - \hbar\omega_s - N\omega_{\rm LO})$ and $\mathbf{k} = \mathbf{k}_e + \mathbf{k}_h = 0$ is the total wave vector of the EHP in the last state before recombination.

For the process of the diagram in Fig. 1(a) all intermediate states of free EHP's are real and the last (excitonic) state is virtual. The absolute value of energy detuning in this virtual state is $|\hbar\omega_s - E_{\rm ex}|$ [see Eq. (13)]. This is also true for the process of Fig. 1(b) where the last excitonic state results in the same resonant factor as in the process of Fig. 1(a). Therefore this process can be understood as the creation of a real exciton, which recombines via an indirect LO-phonon-assisted transition.[16]

To estimate the relative weight of the three types of contributions we have to analyze their dependence on the small parameter of perturbation theory which is the Fröhlich constant α. Equations (4) and (17) are proportional to α^3 within the interval $\omega_l > \omega_g + (N-1)\omega_{\rm LO}$ and for $N \geq 4$. Equation (8) is also proportional to α^3 under the conditions $\omega_l > \omega_{\rm ex} + N\omega_{\rm LO}$ and $N \geq 5$. This means that, for large enough N and ω_l, *all three contributions may be of the same order of magnitude.*

Let us explain the origin of the dependence $\sigma_N \sim \tilde{\alpha}^3$ using Eqs. (12), (14), and (18) for the case of the simplified electron-phonon interaction introduced above Eq. (10). The product $n^Z_{N-1} f^Z_{N-1}(\mathbf{r}=0)$ in Eq. (12) is proportional to $\tilde{\alpha}^2$. Indeed, for $\gamma^Z_e(K_{N-1}) \sim \tilde{\alpha}$ the value n^Z_{N-1} is proportional to $\tilde{\alpha}^{-1}$ and $f^Z_{N-1}(r=0)$ is proportional to $\lambda^{-3} \sim \tilde{\alpha}^3$. Similarly, $n^Z_{N-2} f^Z_{N-2}(\mathbf{r}=0)$ in Eq. (14) is proportional to $\tilde{\alpha}^2$ when $\gamma^Z_e(K_{N-2}) \sim \tilde{\alpha}$. For free EHP's (Ref. 12) the value $n^Z_N(\mathbf{k}=0) f^Z_N(\mathbf{k}=0, \mathbf{r}=0)$ in Eq. (18) is proportional to $\tilde{\alpha}^3$. Taking into account that W^Z_{AN} and W^Z_{BN-1} in Eqs. (12) and (14) are proportional to $\tilde{\alpha}$, that the value of W_C in Eq. (18) is independent of $\tilde{\alpha}$, and that the factor $\gamma^Z_l(K^{\rm ex}_{N-1})/\gamma^Z_{\rm ex}(K^{\rm ex}_{N-1})$ in Eq. (14) is also independent of $\tilde{\alpha}$ above the excitonic resonance, we arrive to the dependence $\sigma_N \sim \tilde{\alpha}^3$ for all three types of contributions. Note that in the range, where $\gamma^Z_e(K_{N-1}) \to \Gamma_e(K_{N-1})$, the product $n^Z_{N-1} f^Z_{N-1}(\mathbf{r}=0)$ is still $\sim \tilde{\alpha}^2$ since $n^Z_{N-1} \sim \Gamma_e^{-1}$ and $f^Z_N(r=0) \sim \Lambda^{-1}\lambda^{-2} \sim \Gamma_e \tilde{\alpha}^2$, where $\Lambda = \hbar K/m_e\Gamma_e$ is the mean free path of the electron with energy less than the energy of LO phonon. The same estimate is valid for $n^Z_{N-2} f^Z_{N-2}(\mathbf{r}=0)$ in Eq. (14) when $\gamma^Z_e(K_{N-2}) \to \Gamma_e(K_{N-2})$ and also for the contribution of free EHP's.[12] The sharp decrease in the inverse electron lifetime $\gamma_e \to \Gamma_e$ in the last real electron state does not lead to any resonances in the scattering efficiency for all three type of processes because of the compensation of Γ_e in the expression for the cross section. This should be physically clear: the gain in the total number of EHP's, which have emitted a given number of LO phonons, is compensated by the decrease in the distribution function of pairs at zero relative distance between electron and hole. Thus, at laser frequencies $\omega_l = \omega_g + N\omega_{\rm LO}$ [point A in Fig. 2(a)] for the contribution of a process in Fig. 1(a) and $\omega_l = \omega_g + (N-1)\omega_{\rm LO}$ [point C in Fig. 2(b)] for the process in Fig. 1(b) the scattering efficiency does not acquire any characteristic feature although the scattering mechanisms for free EHP's go through a drastic change in points B and D where the pair arrives from points A and C after emission of either $(N-1)$ or $(N-2)$ LO phonons, respectively.

Near the outgoing excitonic resonance the energy detuning in the factor $\{(\omega_s - \omega_{\rm ex})^2 + [\gamma_{\rm ex}(0)/2]^2\}^{-1}$ goes to zero and the contribution of diagrams in Figs. 1(a) and 1(b) dominates the MPRRS efficiency. The factor $\gamma^Z_l(K^{\rm ex}_{N-1})/\gamma^Z_{\rm ex}(K^{\rm ex}_{N-1})$ in Eq. (14) is of zero and first order in the coupling constant $\tilde{\alpha}$ above and below the resonance point, respectively. It suffers a drastic increase at the transition $\gamma^Z_{\rm ex}(K^{\rm ex}_{N-1}) \to \Gamma_{\rm ex}(K^{\rm ex}_{N-1})$. *This enhancement is not compensated, in contrast to the above discussed case* $\gamma_e \to \Gamma_e$. Therefore, the contribution of the process in Fig. 1(b) *strongly exceeds* that of Fig. 1(a) below the resonance. The physical reason for this is the following: The number of excitons in the state $K^{\rm ex}_{N-1}$ is drastically increased when $\gamma^Z_{\rm ex}(K^{\rm ex}_{N-1}) \to \Gamma_{\rm ex}(K^{\rm ex}_{N-1})$. At the same time, nothing happens to the distribution of electron and hole with respect to the relative distance since *both are bound* into the discrete state of the exciton.

The dependence of $\gamma_{\rm ex}(K^{\rm ex}_{N-1})$ on ω_l is very important for the form of the outgoing excitonic resonance profile. For $\omega_l > \omega_{\rm ex} + N\omega_{\rm LO}$ the exciton in the state with wave vector $K^{\rm ex}_{N-1}$ can emit a LO phonon in a real transition and $\gamma_{\rm ex}(K^{\rm ex}_{N-1})$ is proportional to α. For $\omega_l < \omega_{\rm ex} + N\omega_{\rm LO}$ the value of $\Gamma_{\rm ex}(K^{\rm ex}_{N-1})$ is determined by the other, less effective scattering mechanisms. The incident light frequency corresponding to the outgoing resonance $\omega_s = \omega_{\rm ex}$ lies exactly at the border of the two intervals. Therefore, the profile of integrated scattering intensity versus ω_l for an Nth-order process must be asymmetric with respect to $\omega_l = \omega_{\rm ex} + N\omega_{\rm LO}$.

Note that in the range $\omega_l < \omega_{\rm ex} + N\omega_{\rm LO}$ the indirect exciton recombination for the process of Fig. 1(b) can be preceded by a number of scattering events with acoustic phonons. In order to account for such contribution we need to know the exciton distribution function $P^{\rm ex}_{N-1}(E)$ which must be spread around the energy $E(K^{\rm ex}_{N-1}) = \hbar\omega_l - E_{\rm ex} - (N-1)\hbar\omega_{\rm LO}$. In the interval $\hbar\omega_{\rm LO} > E(K^{\rm ex}_{N-1}) > \Delta E$ a successive interaction with a number of acoustic phonons may lead to the exciton decay and its exit from the processes forming the distribution $P^{\rm ex}_{N-1}(E)$. The spread of $P^{\rm ex}_{N-1}(E)$ is then much smaller than under condition $0 < E(K^{\rm ex}_{N-1}) < \Delta E$, where a decay due to the interaction with acoustical phonons is impossible. The distribution function $P(E)$ in the interval $0 < E(K^{\rm ex}_{N-1}) < \Delta E$ has been calculated, for instance, in Refs. 20 and 21. However, this region is far enough from the outgoing excitonic resonance which is of primary interest in this paper. To the best of our knowledge, the distribution function has not been calculated in the interval $\hbar\omega_{\rm LO} > E(K^{\rm ex}_{N-1}) > \Delta E$.

To summarize, the combined contributions to the MPRRS cross sections when free EHP bind into the excitons at the last stages of the scattering process have been calculated. They can be of the same order of magnitude as the pure EHP contribution. Near and below the excitonic resonance $\omega_s = \omega_{\rm ex}$ the combined contributions strongly exceed that of free EHP's. The outgoing resonance profile must be asymmetric since crossing the energy $\hbar\omega_l = E_{\rm ex} + N\omega_{\rm LO}$ from above leads to a drastic

increase of the prefactor $\gamma_l^Z(K_{N-1}^{\rm ex})/\gamma_{\rm ex}^Z(K_{N-1}^{\rm ex})$ due to a decrease in $\gamma_{\rm ex}^Z(K_{N-1}^{\rm ex})$.

ACKNOWLEDGMENTS

V.I.B. and S.T.P. thank the European Union, Ministerio de Educación y Ciencia de España (DGICYT) and the Russian Fundamental Investigation Fund (RFIF) (93-02-2362) for financial support and the University of Valencia for its hospitality. I.G.L. and A.V.P. appreciate financial support from RFIF (950204184A). This work has been partially supported by Grant No. PB93-0687 (DGICYT). Thanks are also due to P. P. Kulish for a critical reading of the manuscript.

* On leave from the P.N. Lebedev Physical Institute, Russian Academy of Sciences, Moscow, Russia.

[1] R. C. C. Leite, J. F. Scott, and T. C. Damen, Phys. Rev. Lett. **22**, 780 (1969).

[2] J. F. Scott, R. C. C. Leite, and T. C. Damen, Phys. Rev. **188**, 1285 (1969).

[3] B. Bendow, in *Proceedings of the 1st Soviet-American Symposium. The Theory of Light Scattering in Solids (Moscow) 1975* (Nauka, Moscow, 1975), Vol. 1, p. 328.

[4] S. A. Permogorov, V. V. Travnikov, Fiz. Tverd. Tela (St. Petersburg) **22**, 2651 (1980) [Sov. Phys. Solid State **22**, 1547 (1980)].

[5] K. Nakamura, N. Ohno, M. Yoshida, and Y. Nakai, Solid State Commun. **36**, 211 (1980).

[6] M. Yoshida, N. Ohno, M. Mitsutake, K. Nakamura, and Y. Nakai, J. Phys. Soc. Jpn. **54**, 569 (1985).

[7] K. A. Aristova, C. Trallero Giner, I. G. Lang, and S. T. Pavlov, Phys. Status Solidi B **85**, 351 (1978).

[8] C. Trallero Giner, I. G. Lang, and S. T. Pavlov, Fiz. Tverd. Tela (St. Petersburg) **23**, 1265 (1981) [Sov. Phys. Solid State **23**, 743 (1981)].

[9] C. Trallero Giner, I. G. Lang, and S. T. Pavlov, Phys. Status Solidi B **100**, 631 (1980).

[10] S. T. Pavlov, Dr. Sci. thesis, St. Petersburg State University, St. Petersburg, 1979, p. 290; E. L. Ivchenko, I. G. Lang, and S. T. Pavlov, Fiz. Tverd. Tela (St. Petersburg) **19**, 1751 (1977) [Sov. Phys. Solid State **19**, 718 (1977)]; E. L. Ivchenko, I. G. Lang, and S. T. Pavlov, Phys. Status Solidi B **85**, 81 (1978).

[11] R. Zeyher, Solid State Commun. **16**, 49 (1975).

[12] A. V. Goltsev, I. G. Lang, S. T. Pavlov, and M. F. Bryzhina, J. Phys. C **16**, 4221 (1983).

[13] V. I. Belitsky, A. V. Goltsev, I. G. Lang, and S. T. Pavlov, Zh. Éksp. Teor. Fiz. **86**, 272 (1984) [Sov. Phys. JETP **59**, 155 (1984)].

[14] The strong outgoing resonance observed in a second-order resonant Raman scattering from InP at the $E_0+\Delta_0$ critical point [W. Kauschke and M. Cardona, Phys. Rev. B **33**, 5473 (1986)] has been analyzed within a theoretical model involving free electron-hole pairs [R. Zeyher, Phys. Rev. B **9**, 4439 (1974)] since the exciton binding energy is very small. However, the singularity in the calculated profile is logarithmic rather than Lorentzian. When fitting the data it requires physically unreasonable (too small) values of the broadening parameters. The problem is solved when using excitons as intermediate states (Ref. 15).

[15] A. Garcia-Cristobal, A. Cantarero, C. Trallero Giner, and M. Cardona, Phys. Rev. B **49**, 13 430 (1994).

[16] I. G. Lang, S. T. Pavlov, and A. V. Prokhorov, Fiz. Tverd. Tela (St. Petersburg) **32**, 895 (1990) [Sov. Phys. Solid State **32**, 528 (1990)].

[17] I. G. Lang, S. T. Pavlov, and A. V. Prokhorov, Solid State Commun. **82**, 135 (1992).

[18] I. G. Lang, S. T. Pavlov, A. V. Prokaznikov, and A. V. Goltsev, Phys. Status Solidi B **127**, 187 (1985).

[19] Note that this assumption is reasonable for tetrahedral semiconductors where the electron mass is ten times smaller than the heavy-hole mass. The calculations with a finite value of the hole mass are more complicated and do not change the physical conclusions.

[20] C. Trallero Giner, O. Sotolongo Costa, I. G. Lang, and S. T. Pavlov, Fiz. Tverd. Tela (St. Petersburg) **28**, 2075 (1986) [Sov. Phys. Solid State **28**, 1160 (1986)].

[21] C. Trallero Giner, O. Sotolongo Costa, I. G. Lang, and S. T. Pavlov, Fiz. Tverd. Tela (St. Petersburg) **28**, 3152 (1986) [Sov. Phys. Solid State **28**, 1774 (1986)].